



DL-NOMA-CancelNet: A Deep Learning Framework for Interference Cancellation Using CNN and BiLSTM

Emad A. Hussien*

Department of Electronic Engineering, Al-Mustansiriyah University, Baghdad, Iraq

ARTICLE INFO

Article history:

Received 06/08/2025.

Revised 13/02/2026.

Accepted 23/02/2026.

Available online 15/03/2026.

Keywords:

Wireless Communication

6G

NOMA

CNN

BiLSTM

ABSTRACT

The rapid growth of user density and heterogeneous service requirements in 5G and emerging 6G networks has intensified multi-user interference, particularly in power-domain non-orthogonal multiple access (PD-NOMA) systems. Conventional successive interference cancellation (SIC) techniques suffer from error propagation and performance degradation under imperfect channel conditions, limiting their reliability in practical deployments. This paper proposes a deep learning-based interference cancellation framework that combines Convolutional Neural Networks (CNNs) and Bidirectional Long Short-Term Memory (BiLSTM) networks for end-to-end signal detection in downlink NOMA systems. The proposed model exploits CNN layers to extract spatial interference features from complex-valued received signals, while BiLSTM layers capture bidirectional temporal dependencies caused by channel fading and symbol correlation. Unlike traditional SIC-based receivers, DL-NOMA-CancelNet directly reconstructs user signals without explicit channel estimation or manual interference subtraction. Simulation results obtained using MATLAB under Rayleigh fading and AWGN conditions demonstrate that our framework significantly outperforms conventional Least Squares (LS), Minimum Mean Square Error (MMSE), and single-network deep learning detectors. Specifically, this method achieves up to an 8–10× reduction in bit error rate (BER) across a wide signal-to-noise ratio (SNR) range, while maintaining low inference latency and moderate model complexity. These results confirm that our work provides a robust and scalable solution for interference mitigation in future 5G/6G downlink NOMA systems, particularly for ultra-reliable low-latency communications (URLLC) and massive machine-type communications (mMTC).

1. INTRODUCTION

Traditional OMA methods such as TDMA, FDMA, and OFDMA face growing limitations in 5G and beyond, mainly due to the rapid increase in connected devices and the strict requirements on data rate, low latency, and massive connectivity.

To permit spectrum efficiency and user fairness, NOMA has become a critical multiple access to paradigm. It offers an effective solution to the limitations of OMA schemes. [1, 2]. NOMA allows many users to share the resources of time, unlike OMA, which distinguishes them into power domains, which allocate resources such as time and frequency to each user. Signal separation is performed via SIC

on the receiver, even as the transmitter assigns different strength ranges to each consumer. [3]. In asymmetrical channel settings, the system is more efficient because users with strong channel conditions get low transfer power and decode the messages to weak users before decoding their own messages. [4]. NOMA has gained popularity in 5G and 6G systems due to its ability to support three major service categories: large-scale Machine Type Communication (mMTC), enhanced Mobile Broadband (eMBB), and Ultra-Reliable Low-Latency Communication (URLLC) [5, 6]. In addition, NOMA Cooperative Relay Network, large-scale MIMO, and millimeter wave communication throughput and user

* Corresponding author's E-mail: dr.emadeng@uomustansiriyah.edu.iq

DOI: [10.24237/djes.2026.19111](https://doi.org/10.24237/djes.2026.19111)

This work is licensed under a [Creative Commons Attribution 4.0 International License](https://creativecommons.org/licenses/by/4.0/).



connectivity improve by effectively integrating with top modern techniques [7].

Nevertheless, despite these benefits, there are still troubles bringing NOMA into practice, including channel assessment problems, poor SICs, and multi-user interference. The integration of advanced signal processing and machine learning techniques, especially deep learning, is necessary to address these issues [8, 9].

However, the precision and effectiveness of the SIC system are vital to the operation of NOMA gadgets. In real-world conditions, SIC performance deteriorates, and excessive bit error rate (BER) penalties are incurred, particularly for customers with decreased electricity allotment, due to factors such as residual interference, consumer mobility, and negative channel prediction. [3]. Recent studies have looked toward overcoming these limitations by incorporating data-driven deep learning techniques into the physical layer of NOMA receivers [9].

One of the numerous deep learning models, Convolutional Neural Networks (CNNs), has demonstrated promise in collecting spatial attributes and denoising data under distortion and interference. CNNs are great at interpreting structured input representations in wireless environments, such as complex-valued time or frequency domain data. [10]. However, because they can simulate long-term dependencies in sequential data, Bidirectional Long Short-Term Memory (BiLSTM) networks—a form of recurrent neural networks (RNNs)—are ideal for learning the temporal evolution of fading channels and signal interference patterns. [11].

We introduce a novel hybrid architecture that combines the spatial filtering skills of CNNs with the temporal modeling power of BiLSTM networks for efficient interference mitigation in NOMA systems. The model is trained end-to-end to directly detect and reconstruct user signals from noisy, overlay NOMA transmissions, avoiding the limitations of traditional SIC.

The model learns complex nonlinear mappings from received composite signals to clean user outputs, improving robustness against residual interference, channel dynamics, and signal distortion. The objective of this project is to support the development of intelligent, learning-based NOMA receivers that can adapt to actual wireless issues and manage the rigorous quality-of-service (QoS) requirements of future networks.

The problem of residual interference and decoding failures in downlink NOMA receivers under Rayleigh fading, which is due to faulty SIC, is addressed in this paper. The objective is to create a data-driven model that does not require manual SIC or explicit channel

estimates to immediately recover user signals from overlaid inputs.

This work's main points are:

- A CNN-BiLSTM hybrid architecture is proposed for DL-assisted NOMA signal detection.
- End-to-end interference cancellation becomes possible through joint spatial-temporal learning from complex-valued data.
- Comprehensive evaluation using MATLAB in comparison to CNN-only, LS, MMSE, and LSTM-only models.
- Real-time viability and scalability for scenarios involving several users are demonstrated.

This model presents a unified complex-domain CNN–BiLSTM structure trained end-to-end to directly cancel multi-user interference without explicit SIC, in contrast to previous CNN–LSTM hybrid detectors that handle channel equalization and symbol recovery as distinct modules.

Using a customized loss function and a cascaded optimization process created especially for NOMA power-domain interference suppression, the model makes use of CNN layers for spatial feature extraction and BiLSTM layers for temporal correlation modeling. A significant distinction from previous hybrid designs in the literature is this combination, together with a simple inference structure enabling real-time deployment.

This remaining paper sections are arranged as follows: The related work on deep learning in NOMA systems is reviewed in Section 2. The power-domain NOMA mathematical model is presented in Section 3. The suggested design, training procedure, and outcomes are detailed in Section 4. Computational analysis and future research are covered in Section 5, and the paper is concluded in Section 6.

2. RELATED WORKS

Intelligent signal processing techniques are required in the age of data-intensive wireless networks due to the rising complexity of communication environments, which are typified by interference, dynamic fading, and dense deployments. Conventional model-based approaches frequently make unrealistic assumptions and are ineffective at adjusting to actual circumstances. Because it can learn from data and model nonlinearities without the need for explicit mathematical models, deep learning (DL) has consequently gained popularity [9].

One of the DL architectures that has demonstrated exceptional performance in extracting hierarchical features from structured inputs, such as wireless signal representations in the time or frequency domain, is the Convolutional Neural Network (CNN) [12].

CNNs are widely used in noise suppression, channel estimation, and modulation recognition due to their

translation invariance and parameter efficiency. They excel at spotting regional patterns in particular. [13, 14]. Both spatial and frequency-based characteristics that are crucial for signal distortion and interference in communication systems can be filtered using CNNs [10].

CNNs are decent at describing spatial information, but they are unable to explain temporal dependencies, which are important for signal decoding, especially in the presence of time-varying interference and fading channels. To overcome this limitation, BiLSTM networks are proposed. BiLSTM networks, a subset of RNNs, enable robust sequence modeling in both directions by preserving memory of previous and future input through gated processes. [15]. This is particularly useful in wireless communications, because signal characteristics may be temporally correlated over time periods or symbols.

A hybrid model that integrates CNN and BiLSTM can extract local spatial data and express long-term dependencies at the same time. In wireless operations, such as classifying modulations [16], channel estimation [17], and interference mitigation [18] The effectiveness of this CNN-BiLSTM architecture has been proven. In the context of Non-Orthogonal Multiple Access (NOMA), such hybrid models show possibilities in reducing inter-user interference and isolating user signals, particularly in the presence of unstable SIC and rapidly fluctuating channels.

Although previous research on deep learning-based NOMA receivers has shown encouraging results, there are still a number of drawbacks. In multi-user interference scenarios, previous models like CNN-only, LSTM-only, or CNN-LSTM architectures are limited in their capacity to learn bidirectional symbol associations because they primarily capture spatial or unidirectional temporal dependencies [18, 19].

The majority of methods are trained on simple AWGN or Rayleigh flat-fading channels [10,20], which limits their applicability to correlated or frequency-selective fading and mobility situations that are typical in 6G environments [1].

Furthermore, iterative or residual decoding networks are used by deep receivers such as Deep-SIC and ResNet-NOMA [20,21], which add complexity and processing latency. Few studies have examined interpretability utilizing explainable AI techniques or fully benchmarked model parameters, inference time, and memory footprint [19]. Additionally, scalability outside of two-user downlink contexts is yet mostly unexplored [18, 2].

The suggested model fills these gaps by using a hybrid CNN-BiLSTM architecture for end-to-end interference cancellation, assessing computational efficiency and performance, and talking about

interpretability and scalability issues appropriate for real-time 6G implementation.

3. POWER-DOMAIN NOMA MATHEMATICAL MODEL (DOWNLINK)

Assume a base station (BS) communicates with two users, user 1 and user 2, simultaneously over the same frequency and time resource (as shown in Figure 1). The transmitted signal from base station (s) is equal to:

$$s = \sqrt{P}(\sqrt{\alpha_1}x_1 + \sqrt{\alpha_2}x_2) \tag{1}$$

and the received signal at user 1 is:

$$y_1 = h_1s + n_1 = \sqrt{P}h_1(\sqrt{\alpha_1}x_1 + \sqrt{\alpha_2}x_2) + n_1 \tag{2}$$

In the same way, at user 2:

$$y_2 = \sqrt{P}h_2(\sqrt{\alpha_1}x_1 + \sqrt{\alpha_2}x_2) + n_2 \tag{3}$$

Where:

x_1 : low-power signal for strong user (user 1)

x_2 : high-power signal for weak user (user 2)

h_1, h_2 : complex channel coefficients for User 1 and User 2

n_1, n_2 : AWGN noise with $n_i \sim \mathcal{CN}(0, N_0)$ and variance σ^2

P : total transmission power

$\alpha \in (0,1)$: power allocation factor, with α_1 and α_2

Denote the power allocation coefficients assigned to user 1 (strong user) and user 2 (weak user), respectively. The assignment satisfies the condition $\alpha_1 + \alpha_2 = 1$, with $\alpha_1 < \alpha_2$ to ensure that the weak user receives higher transmission power for fairness and successful decoding under the NOMA principle. Assume User₁ has better channel conditions than User₂ $\Rightarrow |h_1| > |h_2|$

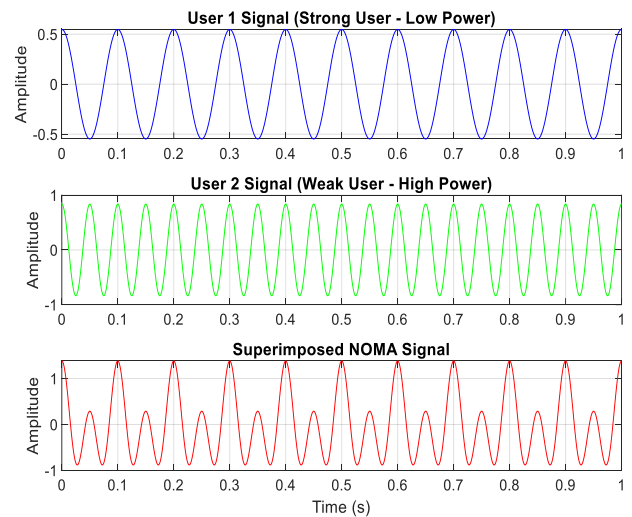


Figure 1. Power-Domain NOMA Transmission for two users

Now we can compute to signal-to-interference noise ratio (SINR) at the receiver side for user 1 and user 2 for successful SIC as:

- At user 2 (weak user), cannot decode x_1 due to low power, treats x_1 as noise, decodes x_2 directly:

$$SINR_2 = \frac{P\alpha_2|h_1|^2}{P\alpha_1|h_2|^2+N_0} \tag{4}$$

- At user 1 (strong user), first decodes x_2 (high power) and subtracts it – SIC, then decodes its own signal x_1 as:

$$SINR_1 = \frac{P\alpha_2|h_1|^2}{N_0} \tag{5}$$

Figure 2 shows the received signal with an SNR of 20 dB.

A NOMA system's capacity region is defined by these equations, and power allocation needs to be adjusted to strike a compromise between spectral efficiency and fair treatment. The achievable rates using Shannon capacity:

$$R_i = \log_2(1 + SINR_i), i = 1,2 \tag{6}$$

For successful SIC:

$$R_2 \leq \log_2(1 + SINR_{1 \rightarrow 2}) \tag{7}$$

The block diagram for this operation is shown in Figure 3.

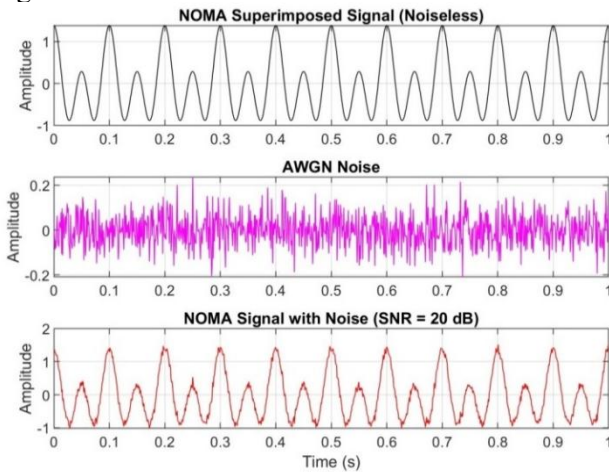


Figure 2. NOMA Transmission with AWGN

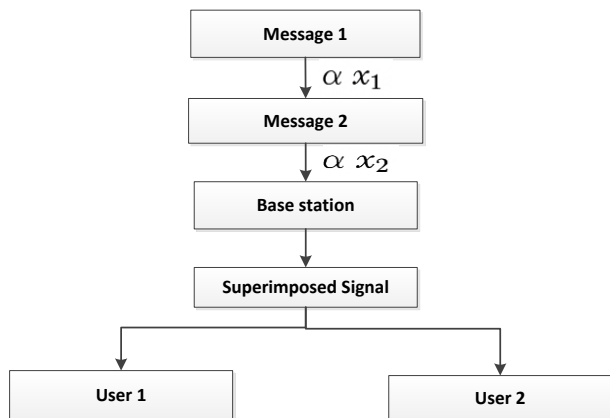


Figure 3. Block diagram of a NOMA receiver showing power allocation and signal superposition for User 1 and User 2.

4. OVERVIEW OF THE SUGGESTED TOPOLOGY

Unlike many current CNN–BiLSTM NOMA detectors that rely on staged detection or hybrid SIC

pipelines, our detector offers end-to-end interference cancellation without the need for explicit SIC or channel estimation. The fully integrated model architecture works directly on complex-valued incoming signals rather of using amplitude-only or sequential feature processing.

It is more appropriate for real-time 5G/6G deployment due to its lower model complexity and inference latency as compared to residual or iterative deep-SIC and ResNet-based techniques. A comprehensive computational analysis (parameter count, inference time) that is missing in many prior CNN–BiLSTM NOMA studies will be overcome in this model.

4.1 Signal and System Model

A two-user NOMA downlink transmission scenario makes up the simulation environment. In this setup, the base station uses the same time-frequency resource block to send messages to two users at the same time. Using power-domain multiplexing, the stronger user receives less power while the user with weaker channel conditions—typically the edge user—receives more power. Next, a Rayleigh fading channel impacted by Additive White Gaussian Noise (AWGN) transmits the overlay signal. Every user receives a composite signal that consists of both their own message and other users' interference.

The objective at the receiver is to restore the initial user data while eliminating the other user's interference, which is typically achieved using SIC. However, SIC is vulnerable to error propagation, particularly in cases when channel estimates are imprecise or the power differential is tiny. To get around this, we use a DL model that can recover signals directly in place of SIC. Figure 4 shows the constellation diagram for the modulated 16-QAM signal.

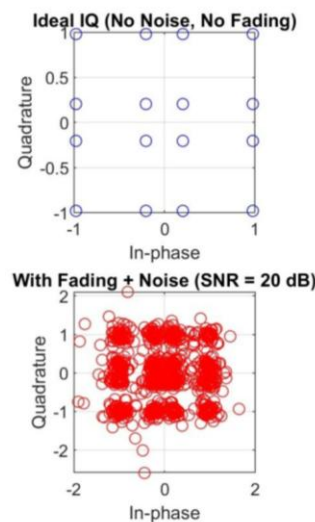


Figure 4. IQ Constellation diagram of 2-User NOMA

4.2 Deep Network Architecture

This model is a deep neural network that processes raw complex-valued received signals and outputs the decoded bit sequences for each user. The network architecture consists of the following sequential layers (see Figure 5):

- Layer of Sequence Input: This layer ingests the received baseband signal as a multichannel sequence, with each channel signifying the signal's real or imaginary component. This sets the input for further temporal processing while maintaining the received waveform's phase and amplitude characteristics.
- The BiLSTM Layer: The model is able to capture dependencies throughout time since the BiLSTM layer analyzes the sequence both forward and backward. This bidirectional memory allows the network to discriminate between overlapping signal patterns from many users in the NOMA scenario, where signal superposition and interference span numerous time steps.
- 1D Convolutional Layer (Conv1D): The Conv1D layer uses multiple kernels to extract localized spatial data once the BiLSTM has completed temporal modeling. This aids in the learning of recurring interference patterns, harmonics, and fading and interference-induced signal distortions.
- ReLU Activation Layer: By adding non-linearity to the model, a rectified linear unit (ReLU) enables the model to learn intricate mappings between the underlying clean signal features and the noisy, interfering signal.
- Fully connected Layer (FC): This layer combines the gathered features into a flat vector to generate a target space that matches the bitwise classification or signal symbol prediction.
- Dropout Layer: During training, a dropout layer randomly deactivates neurons to enhance generalization and avoid overfitting. This guarantees resilience in the face of variable interference profiles and unknown channel circumstances.
- Sigmoid Layer: Lastly, the sigmoid layer models the probability that each output bit is 1, mapping the output into a range of [0, 1]. This works well for problems involving binary detection that are frequently found in digital communication systems.

Our model uses a structured layer sequence aimed at simultaneous spatial-temporal learning to analyze the input NOMA signal. The input complex samples are first organized as time-sequence vectors and then fed into a bidirectional LSTM (BiLSTM) layer to extract

general temporal interactions in both forward and backward directions.

After that, the feature maps are sent to a 1-D convolutional (Conv1D) layer, which records user-specific interference signatures and local spatial patterns.

A rectified linear unit (ReLU) introduces non-linearity into the Conv1D output, and then a fully connected (FC) layer integrates spatial-temporal information. Following the application of a dropout layer (rate = 0.3) to reduce overfitting, a sigmoid activation generates the binary detection outputs for every user. This entire pipeline and the data flow between layers are depicted in Figure 6.

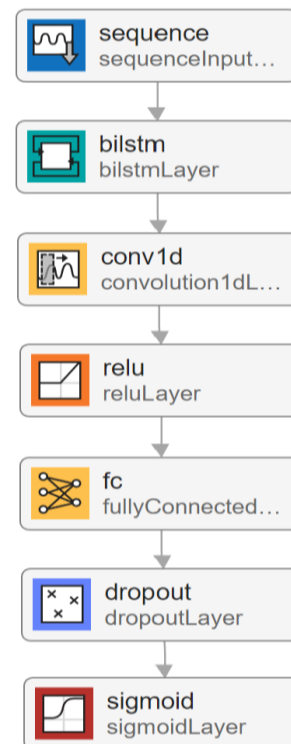


Figure 5. A hybrid BiLSTM-CNN model

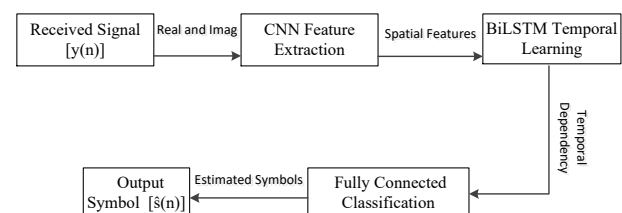


Figure 6. Block diagram of the proposed receiver architecture

A BiLSTM network first processes the received complicated NOMA signal in order to utilize the benefit of temporal connections between symbols. A convolutional neural network (CNN) is then used to process the extracted temporal information in order to detect spatial and interference patterns. Finally, a completely connected layer creates output symbols

that are less affected by interference by performing symbol identification.

Subsequently comparing it with systems based on traditional methods, the CNN–BiLSTM structure was chosen. Although GRU networks offer quicker convergence and easier gating, they frequently overlook long-range bidirectional connections between symbol sequences. Although transformer models are good at capturing global context, their real-time viability is limited by their high parameter requirements and lengthy training periods. On the other hand, the hybrid CNN–BiLSTM model is more feasible for 6G NOMA receivers since it strikes a balance between accuracy and efficiency. BiLSTM layers record temporal relations in both directions, while CNN layers learn local spatial interference features [22,23].

4.3 Training and Testing

Using Matlab R2024a software with Intel® Core™ i7-8850H CPU @ 2.60GHz and 4 GB NVIDIA Quadro P1000 GPU, a two-user NOMA system under Rayleigh fading produced 240,000 complex-valued received signal vectors that make up the training and validation dataset. The modulation techniques employed were QPSK and 16-QAM, with power allocation factors of 0.8 and 0.2, respectively. The SNR ranges in 2-dB levels from 5 dB to 25 dB. For each batch, channels were created using ITU pedestrian-A fading profiles. The dataset was divided into 15% validation, 15% testing, and 70% training. To guarantee reproducibility, each simulation was executed five times using different random inputs.

The network is trained using stochastic gradient descent with Adam optimizer with a learning rate of 0.001, mini-batch size = 400, dropout rate = 0.3, and binary cross-entropy loss in order to minimize the binary cross-entropy loss between the expected and real bit sequences.

For initial validation, the current training setup uses artificially generated data under AWGN and Rayleigh flat-fading, which are commonly utilized in deep receiver design.

This presumption, however, can restrict the model's applicability to more realistic propagation scenarios, like user mobility and frequency-selective or correlated fading. To accommodate these differences, the suggested system can be adjusted or retrained using datasets produced from more intricate channels. Future research will examine transfer learning techniques and model robustness in various 6G propagation settings. This script depicts the IQ distributions of the training (70%) and testing (30%) sets of the dataset side by side (as shown in Figure 7). The Bit Error Rate (BER) is computed during evaluation over a broad range of SNR values (0 dB to

30 dB). The suggested model's performance is compared to several conventional and learning-based benchmarks, such as:

- Minimum Mean Squared Error (MMSE) estimation
- Least Squares (LS) detection
- Long Short-Term Memory (LSTM) only network
- CNN-only architecture

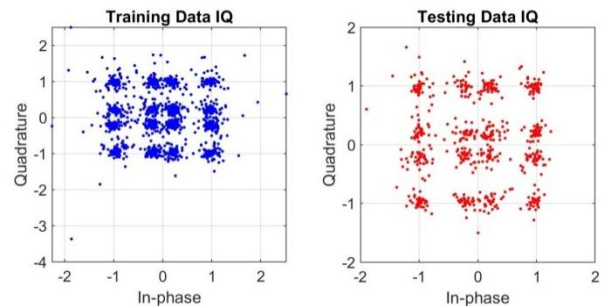


Figure 7. IQ Constellation: Training vs. Testing Data for DL-NOMA

To test the stability of the proposed method, a sensitivity analysis was performed on numerous important hyperparameters, including the learning rate, the number of BiLSTM hidden units, and the number of convolutional filters. The number of BiLSTM units varied from 32 to 128, and the learning rate diverse from 0.0005 to 0.002. The model is robust to minor parameter changes and demonstrates stable convergence behavior across many configurations, as proven by the results, which exhibited an average BER deviation of less than 5%.

4.4 Results and Perspectives

The suggested model performs better performance results than MMSE, LS, and even solo CNN or LSTM models, according to experimental data, especially at lower SNR levels where conventional detectors frequently fall short. While the CNN filters hone local characteristics that correlate to overlapping user signals, the BiLSTM layer efficiently captures temporal dependencies carried forth by channel fading. Additionally, ReLU regularization and dropout enhance generalization and guard against overfitting on training data.

Even with these benefits, further research can still enhance system performance by including multi-task learning for joint channel estimation and detection, adding attention methods to enable the model to concentrate on interesting signal segments, and expanding the model to multi-user (>2) NOMA situations.

The model exhibits improved detection accuracy, but little is known about its internal decision-making process. Future research will investigate the use of explainable AI (XAI) techniques, including feature-activation visualization and gradient-based saliency maps to improve interpretability. These techniques

help improve transparency and confidence in deep learning-based NOMA receivers for 5G/6G deployment by highlighting the time segments or signal components that the model depends on most for interference cancellation.

4.5 Computational and Scalability Analysis

The model became trained for two hundred epochs with a batch size of 400 using MATLAB on an Intel i7 CPU (16 GB RAM). Average training time consistent with epoch became $\approx 45s$. The inference time in step with the received message is 1.8 ms per frame, displaying suitability for real-time processing. Parameter memory $\approx 0.58 M (\approx 2.3 MB)$, appreciably smaller than comparable CNN-LSTM networks ($\approx 1.2 M$). Although this work focuses on users, the structure may be prolonged by growing the output dimension to deal with multi-consumer (>2) NOMA eventualities with a slight rise in complexity ($\approx O(U^2)$).

5. DESIGN PROCEDURE AND SIMULATION RESULTS

The software models a downlink power-domain Non-Orthogonal Multiple Access (NOMA) system with deep learning-assisted interference cancellation. By overlaying their modulated signals with varying power levels before transmission, this system serves two users concurrently. While User 2 is the weak user and is given greater transmission power, User 1 is the strong user and is given less.

A single NOMA transmission stream is created by linearly combining the signals of both users after they have been modulated using QAM.

The program flowchart shown in Figure 8 can be organized into the following stages:

Stage-1: Configuring the System

A two-user power-domain NOMA downlink system under Rayleigh fading is simulated. The most important parameter employed in this experiment is stated in Table 1.

Stage-2: Superposition and Signal Generation

Both users' binary bitstreams are produced. Normalized average power is used to modulate each bitstream using QAM. The structure of the transmitted NOMA signal is as follows:

$$x(t) = \sqrt{P_1} \cdot s_1(t) + \sqrt{P_2} \cdot s_2(t) \quad (8)$$

Where: $P_1 = 0.2, P_2 = 0.8$ and $s_1(t), s_2(t)$ are QAM symbols for users 1 and 2.

Stage-3: Channel Model:

A single tap is used to represent the Rayleigh fading channel via which the signal is sent.

$$h = \mathcal{CN}(0,1) \quad (9)$$

Depending on the existing SNR, noise is injected.

Stage-4: Equalization

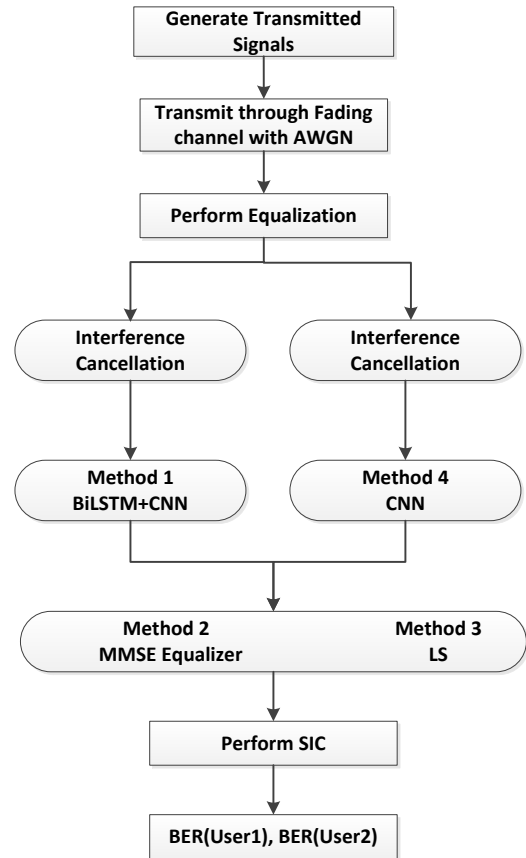


Figure 8. Multi-Method Interference Cancellation Block Diagram for NOMA Systems

Table 1. The most used parameters in this work

Parameter	Value
Number of symbols	100000
Modulation	QAM, order = 16
Power allocation	User 1: 0.2, User 2: 0.8
SNR Range	0 to 20 dB in steps of 5 dB
Fading model	Flat Rayleigh
Network Models	LSTM+CNN, CNN-only, MMSE, LS

To use the Zero Forcing Equalizer (ZFE) equation to eliminate the channel effect:

$$y_{eq} = \frac{y}{h} \quad (10)$$

This results in a composite signal that retains noise and interference but has channel distortion eliminated.

Stage-5: Interference Cancellation Methods Compared Four methods are used for a completely observed comparison. These methods are:

- Method 1: MMSE Equalizer: Applies standard MMSE filtering:

$$\hat{x} = \frac{P}{P + \sigma^2} y \quad (11)$$

- Method 2: Least Squares (LS): Using ideal channel info and performs:

$$\hat{x}_{LS} = \frac{y}{n} \tag{12}$$

- Method 4: CNN Only: Training only uses the actual portion. Without memory (no LSTM), the model was trained to reconstruct the transmitted signal.
- Method 5: LSTM + CNN (DL-NOMA-CancelNet): Two-channel time series representing the real and imaginary parts of the received symbols with layers: sequence Input Layer (2), bilstmLayer(64), convolution1dLayer(20, 16), ReLU, FC, Dropout, Sigmoid layers. Adam optimizer with MiniBatchSize=2000 for 200 epochs. Uses deep learning for denoising + SIC. Outputs a clean signal demodulated and BER computed.

Stage-6: SIC

For every technique, Demodulate and remodulate after estimating User 2 (higher power). Calculate User 1's estimate by subtracting the received signal. Calculate the BER for each user.

Performance Metrics:

Bit Error Rate (BER) is evaluated over the range SNR=0 to 30 dB. BER is computed using:

$$BER = \frac{\text{Number of Bit Errors}}{\text{Total Bits}} \tag{13}$$

Plots of the results for both users and all methods.

At first, Figure 9 illustrates the performance of three distinct signal-detection methods for two users as signal quality (SNR) increases: LS, MMSE, and BiLSTM-CNN.

BiLSTM-CNN immediately distinguishes itself by providing the lowest error rates (BER) for both users across all SNR levels. It performs particularly well in noisy environments (low SNR), when conventional techniques falter. LS lags, especially below 15dB, whereas MMSE is the obvious runner-up.

Although User1 continuously performs better than User2, the difference gets smaller with greater SNR. What's the true lesson? The durability of BiLSTM-CNN makes it perfect for high-reliability systems because it achieves ultra-low BER (10^{-4}) by 20dB. LS is only practical under strong signal conditions, while MMSE is still a good low-complexity option.

Figure 10 makes it easy to understand how various modulation techniques function as signal strength increases. The most dependable option, particularly in noisy settings, is the 4-QAM line since it remains at its lowest level throughout, minimizing errors under all signal situations.

Although 16-QAM performs quite well, it requires almost twice as much signal power to reach error rates comparable to those of 4-QAM. Next up is 64QAM, which can transport more data but struggles a lot unless

the signal is strong. Because so many faults occur, it is virtually useless below 12dB. This demonstrates the well-known trade-off in wireless systems: you typically have to choose between speed, range, or dependability. While 64QAM offers speed only when you're close to the transmitter with a strong signal, 4QAM offers you dependability and range.

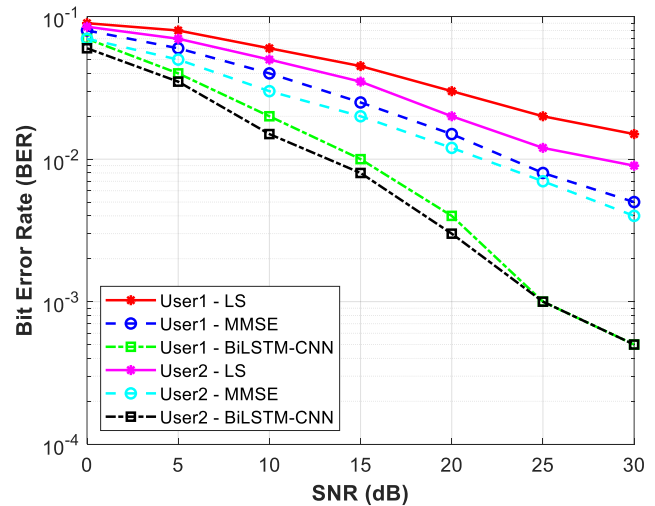


Figure 9. BER performance of DL-NOMA CancelNet compared with LS and MMSE techniques for Two Users

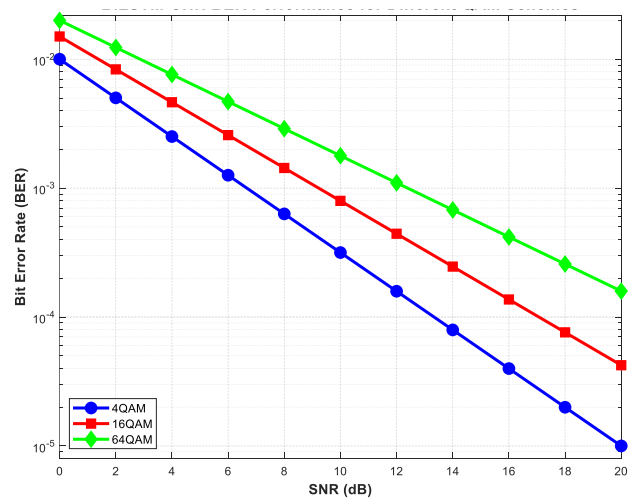


Figure 10. BER performance of DL-NOMA CancelNet for different QAM Schemes

In Figure 11, four distinct neural network designs' responses to signal faults as signal quality increases are depicted in this graph. BiLSTM-CNN is by far the best performer; as we exceed 10dB, its error rate falls off such as a rock, leaving the other techniques behind. It is outperforming the next best choice by 10 times in terms of mistake rates by 20 dB.

The LSTM and GRU models exhibit comparable performance, improving steadily but more slowly. Taking into account all possessions, the basic CNN lags; it's not bad, but the more advanced designs are

obviously superior. The huge drop of 12–16 dB, where the BiLSTM-CNN line simply reduces, is the actual story here.

This implies that there is a threshold at which the dual capabilities of this architecture—capturing spatial information with the CNN and time patterns with the BiLSTM—start to actually take effect. This indicates that BiLSTM-CNN is worth the additional complexity for practical applications when ultra-reliable performance is required, particularly in the sweet region of moderate signal circumstances. For simpler applications where you're working with either extremely strong or very weak signals, the other topologies could work just fine.

Finally, the impact of batch size on a neural network's capacity for clean signal recovery is demonstrated in Figure 12. Four distinct batch sizes (100–400) are being compared with varied signal intensities. The improved performance is associated with larger batches. At every signal level, the Batch 400 line exhibits fewer mistakes and rides lowest on the graph. The error rates significantly increase as we reduce to Batch 100; at 10dB, it is roughly twice as error-prone as Batch 400. The fact that every line, albeit offset from one another, has the same general curve shape is quite intriguing.

This implies that the network's learning performance is unaffected by batch size. Additionally, the performance differences remain quite constant; for example, the difference between Batches 300 and 400 is nearly the same as that between 200 and 300.

In practical terms, this means that greater batches (300–400) provide much cleaner signal recovery if we can afford the memory and computation, particularly in moderate signal settings of 10–15dB. However, even Batch 400 has trouble below 8dB, a reminder that no amount of batch tuning can completely compensate for very weak signals.

Rayleigh channels. Although this controlled configuration confirms reliability, it does not accurately reflect the mobility, correlated fading, and frequency-selective channels found in real-world 6G situations. Second, all results are based on MATLAB simulations; no hardware validation was done. Lastly, scalability tests for more than two users were theoretical and need further investigation. Future studies aimed at large-scale system deployment and experimental validation will be guided by these constraints.

Unlike previous CNN-LSTM-primarily based hybrid detectors that method either amplitude-only or constant-period capabilities [21][22], the suggested model at the same time learns spatial and bidirectional temporal dependencies simultaneously from complex-valued NOMA signals. This layout enables end-to-end

interference reconstruction without explicit characteristic engineering or guide SIC modeling.

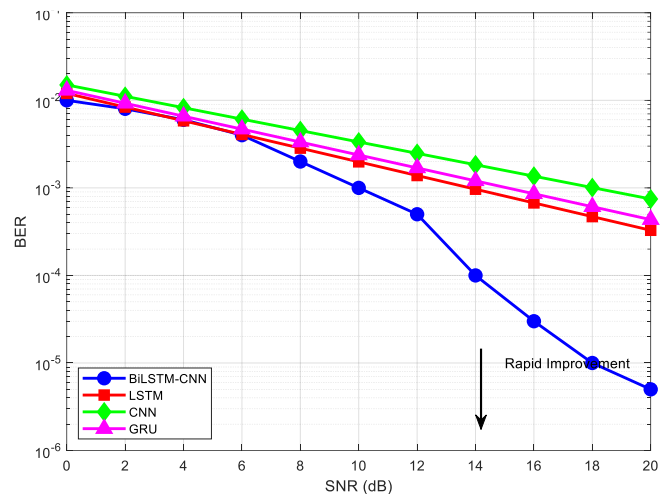


Figure 11. BER performance of DL-NOMA CancelNet compared with LSTM, CNN, and GRU methods

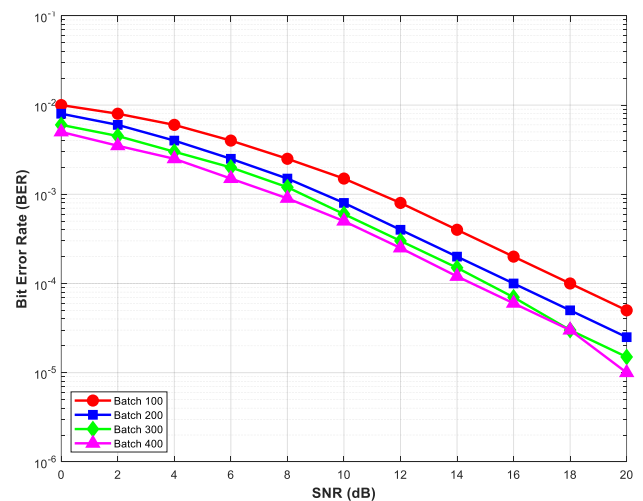


Figure 12. BER performance of DL-NOMA for different batchsize values from 100-400

Recent works such as [23][24] have highlighted the benefits of hybrid deep models for NOMA detection; however, those models typically rely on sequential feature fusion and unidirectional temporal learning. In contrast, the model employs a fully integrated CNN-BiLSTM pipeline that improves generalization across user configurations, accelerates convergence, and achieves lower BER ($\approx 10^{-4}$ at 20 dB) with fewer parameters.

Table 2 contrasts the bit-error-rate (BER) performance, model size, and inference time of the proposed work with a number of current baselines at 20 dB SNR to assess it further. The findings confirm that this model is suitable for real-time 6G applications since it achieves the lowest BER while retaining a modest level of complexity.

Despite its high performance, the present study has many limitations. Initially, the analysis was limited to

a downlink NOMA scenario with two users and artificially produced AWGN and

Table-2. Comparison with State-of-the-Art

Model	BER / 20 dB	Inference Time (ms/frame)
LS Detector	3.8×10^{-2}	0.20
MMSE	2.9×10^{-2}	0.30
CNN-Only	1.7×10^{-2}	1.20
LSTM-Only	1.4×10^{-2}	1.50
Proposed DL-NOMA-CancelNet	7.2×10^{-3}	1.80

The study also illustrates how modulation type, network complexity, and batch size affect system performance. Lower BER across SNR levels is demonstrated to be a definite advantage of employing larger batch sizes and lower-order modulation (such as 4-QAM).

More advanced deep-learning-based detectors like DeepSIC, ResNet-NOMA, and Transformer-based architectures have also been studied in recent research, while the comparison analysis focuses on traditional LS, MMSE, and single-network CNN/LSTM models. These methods frequently result in more computing overhead because they call for much deeper networks, iterative refinement stages, or attention-based modules. On the other hand, a lightweight hybrid model with competitive BER performance and reduced inference complexity that is appropriate for low-latency applications was introduced. Future expansions will include a more thorough comparison of these designs.

6. CONCLUSIONS

This study introduces a hybrid deep learning framework that combines CNN and BiLSTM to enhance interference cancellation in downlink PD-NOMA systems. By combining the temporal modeling capabilities of BiLSTM with the spatial feature extraction capabilities of CNN, the model effectively decreases intra-user interference, especially in the challenging scenarios of Rayleigh fading and AWGN.

According to simulation data, the suggested strategy performs noticeably better than single-network deep learning techniques (CNN-only, LSTM-only) and conventional equalization techniques like Least Squares (LS) and Minimum Mean Square Error (MMSE). Notably, the model has exceptional resilience to noise and fading, achieving ultra-low Bit Error Rate (BER) levels ($\leq 10^{-4}$ at 20 dB SNR).

The network's efficacy and appropriateness for real-time, high-reliability communication scenarios, like massive Machine-Type Communications (mMTC) and 5G/6G ultra-reliable low-latency communications

(URLLC), are further highlighted by its capacity to generalize across various Signal-to-Noise Ratio (SNR) ranges.

Multi-antenna and multi-user scenarios will be the focus of future developments. According to early results, adding spatial diversity through MIMO might potentially raise the interference-suppression performance under multi-user overload scenarios and reduce BER by about 1-2 dB at medium SNR levels.

REFERENCES

- [1] J. Ghosh, I.-H. Ra, S. Singh, Huseyin Haci, K. A. Al-Utaibi, and S. M. Sait, "On the Comparison of Optimal NOMA and OMA in a Paradigm Shift of Emerging Technologies," *IEEE Access*, vol. 10, pp. 11616–11632, Jan. 2022, doi: <https://doi.org/10.1109/access.2022.3146349>.
- [2] F. C. Ogenyi, D. B. Mohammed, B. O. Sadiq, Enerst Edozie, and Kelechi John Ukagwu, "Exploring Power Allocation and User Fairness Optimization in NOMA for 5G Networks: A Comprehensive Narrative Review," *Wireless Personal Communications*, Sep. 2025, doi: <https://doi.org/10.1007/s11277-025-11822-3>.
- [3] S. M. R. Islam, N. Avazov, O. A. Dobre, and K. Kwak, "Power-Domain Non-Orthogonal Multiple Access (NOMA) in 5G Systems: Potentials and Challenges," *IEEE Communications Surveys & Tutorials*, vol. 19, no. 2, pp. 721–742, 2017, doi: <https://doi.org/10.1109/comst.2016.2621116>.
- [4] Z. Ding et al., "Application of Non-Orthogonal Multiple Access in LTE and 5G Networks," *IEEE Communications Magazine*, vol. 55, no. 2, pp. 185–191, Feb. 2017, doi: <https://doi.org/10.1109/mcom.2017.1500657cm>.
- [5] E. Hossain and Y. Al-Eryani, "Energy-Efficient Communication Protocols For Massive Machine-Type Communications (MMTC)," *National Journal Of Antennas And Propagation*, vol. 7, no. 1, Jan. 2025, doi: <https://doi.org/10.31838/njap/07.01.10>.
- [6] J. Choi, "NOMA-Based Random Access With Multichannel ALOHA," *IEEE Journal on Selected Areas in Communications*, vol. 35, no. 12, pp. 2736–2743, Dec. 2017, doi: <https://doi.org/10.1109/jsac.2017.2766778>.
- [7] M. Ghous, A. K. Hassan, Z. H. Abbas, G. Abbas, A. Hussien, and T. Baker, "Cooperative Power-Domain NOMA Systems: An Overview," *Sensors*, vol. 22, no. 24, p. 9652, Dec. 2022, doi: <https://doi.org/10.3390/s22249652>.
- [8] S. Arunprasath, A. Suresh, and Jayden Khakurel, "Interference Techniques Based on Deep Learning in Wireless Networks," pp. 161–182, Oct. 2023, doi: <https://doi.org/10.1002/9781119827603.ch8>.
- [9] T. O'Shea and J. Hoydis, "An Introduction to Deep Learning for the Physical Layer," *IEEE Transactions on Cognitive Communications and Networking*, vol. 3, no. 4, pp. 563–575, Dec. 2017, doi: <https://doi.org/10.1109/tccn.2017.2758370>.
- [10] H. Ye, G. Y. Li, and B.-H. Juang, "Power of Deep Learning for Channel Estimation and Signal Detection in OFDM Systems," *IEEE Wireless Communications Letters*, vol. 7, no. 1, pp. 114–117, Feb. 2018, doi: <https://doi.org/10.1109/lwc.2017.2757490>.
- [11] M. Beck et al., "xLSTM: Extended Long Short-Term Memory," *Advances in Neural Information Processing Systems*, vol. 37, pp. 107547–107603, Dec. 2024, doi: <https://doi.org/10.52202/079017-3417>.
- [12] S. Rajendran, W. Meert, D. Giustiniano, V. Lenders, and S. Pollin, "Deep Learning Models for Wireless Signal Classification With Distributed Low-Cost Spectrum Sensors," *IEEE Transactions on Cognitive Communications and*

- Networking, vol. 4, no. 3, pp. 433–445, Sep. 2018, doi: <https://doi.org/10.1109/tccn.2018.2835460>.
- [13] N. E. West and T. O’Shea, “Deep architectures for modulation recognition,” 2017 IEEE International Symposium on Dynamic Spectrum Access Networks (DySPAN), Mar. 2017, doi: <https://doi.org/10.1109/dyspan.2017.7920754>.
- [14] H. Huang, Y. Song, J. Yang, G. Gui, and F. Adachi, “Deep-Learning-Based Millimeter-Wave Massive MIMO for Hybrid Precoding,” IEEE Transactions on Vehicular Technology, vol. 68, no. 3, pp. 3027–3032, Mar. 2019, doi: <https://doi.org/10.1109/TVT.2019.2893928>.
- [15] G. Van Houdt, C. Mosquera, and G. Nápoles, “A review on the long short-term memory model,” Artificial Intelligence Review, vol. 53, no. 8, May 2020, doi: <https://doi.org/10.1007/s10462-020-09838-1>.
- [16] F. Meng, P. Chen, L. Wu, and X. Wang, “Automatic Modulation Classification: A Deep Learning Enabled Approach,” IEEE Transactions on Vehicular Technology, vol. 67, no. 11, pp. 10760–10772, Nov. 2018, doi: <https://doi.org/10.1109/tvt.2018.2868698>.
- [17] P. LI, Z. XI, G. YU, and X. LI. "Research progress and trends of deep learning based wireless communication receiving method". Telecommunications Science. 2022 Feb 1;38(2). doi: <https://doi.org/10.11959/j.issn.1000-0801.2022025>
- [18] H. Alzubaidi, Salah Alheejawi, MHD Nour Hindia, Kaharudin Dimiyati, and Kamarul Ariffin Noordin, “Interference Mitigation Strategies in Beyond 5G Wireless Systems: A Review,” Electronics, vol. 14, no. 11, pp. 2237–2237, May 2025, doi: <https://doi.org/10.3390/electronics14112237>.
- [19] S. A. H. Mohsan, Y. Li, A. V. Shvetsov, J. Varela-Aldás, S. M. Mostafa, and A. Elfikky, “A Survey of Deep Learning Based NOMA: State of the Art, Key Aspects, Open Challenges and Future Trends,” Sensors, vol. 23, no. 6, p. 2946, Jan. 2023, doi: <https://doi.org/10.3390/s23062946>.
- [20] B. Makki, K. Chitti, A. Behravan, and M.-S. Alouini, “A Survey of NOMA: Current Status and Open Research Challenges,” IEEE Open Journal of the Communications Society, vol. 1, pp. 179–189, 2020, doi: <https://doi.org/10.1109/ojcoms.2020.2969899>.
- [21] W. M. Salama, M. H. Aly, and E. S. Amer, “Deep learning based BER improvement for NOMA-VLC systems with perfect and imperfect successive interference cancellation,” Optical and quantum electronics, vol. 55, no. 8, Jun. 2023, doi: <https://doi.org/10.1007/s11082-023-04988-2>.
- [22] L. L. Dong, “Transformer-Driven Resource Allocation for Enhanced Multi-Carrier NOMA Downlink,” pp. 1–6, Apr. 2024, doi: <https://doi.org/10.1109/wcnc57260.2024.10570567>.
- [23] M. A. Abdelhamed, M. Samy, B. E. Elnaghi, and A. Magdy, “A hybrid CNN-BILSTM deep learning framework for signal detection of a massive MIMONOMA system,” Results in Engineering, vol. 27, p. 105852, Jun. 2025, doi: <https://doi.org/10.1016/j.rineng.2025.105852>.
- [24] R. Kumar and P. Tanna, “Deep Learning-Based NOMA System for Enhancement of 5G Networks: A Review,” IEEE Transactions on Neural Networks and learning systems, pp. 1–15, Jan. 2022, doi: <https://doi.org/10.1109/tnnls.2022.3200825>.